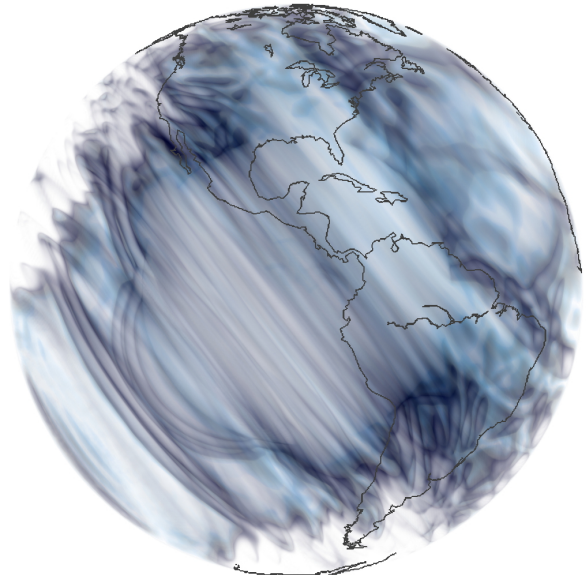


7 Numerical methods for transient elastodynamics: Weak form, finite differences, finite elements and finite volumes



Global seismic wavefield of the Kamchatka event 2013 ($Mw 8.3$ at 611 km depth), numerically calculated by a spectral-element method.

Introduction

As we have seen in the previous lectures, complex media quickly lead to a system of equations which is not analytically or asymptotically solvable in general. In this section, we will introduce three prominent numerical methods: *finite differences* (FD), *finite elements* (FE), and *finite volumes* (FV).

All of these are based upon some gridded discretization of the wave equation and a functional representation upon these grids. Note that, strictly speaking, all methods we ever employ to plot seismograms upon a discrete set of points are “numerical” in nature, and some of the previously introduced methods such as normal-mode summation have important numerical aspects (root-finding of the discrete eigenfrequencies), although they are usually labeled “reference”, or “(quasi-)analytical”.

In the following, we will introduce basic concepts of numerical methods, such as convergence and numerical costs. We will distinguish between the strong and weak form of the equations of motions, and shortly discuss the most prominent numerical methods concerning their flexibility in modeling wave propagation in complex media.

Learn objectives

- You can describe the three main numerical methods presented here (FD, FE and FV).
- You know how temporal and spatial discretizations are achieved.
- You are able to suggest an appropriate numerical approach for different media and problem setups.

7.1 Numerical modeling of seismic wave propagation

While the distinction is blurry, *fully* numerical methods are often seen as follows:

- *Meshing*: Divide domain into a discrete grid which resolves the frequencies of the propagating wave.
- *Discretization*: Define a functional representation upon these grid points.
- *Solving (forward problem)*: Define (local) spatial & temporal differential and integral operators as propagators.

This makes these techniques computationally very demanding since wavefield, media, and grid properties need to be known locally. The advantage of course is the ability of honoring local media variations.

Convergence

The three methods we introduce here converge to the analytical solution when increasing grid resolution for fixed waves, and as such have similar properties to all other methods (reflectivity, mode summation) which also need a certain parameter framework to yield precise solutions. They may be more accurate for certain parts of the solution, e.g. body waves compared to dispersive surface waves. The order of convergence depends on the numerical discretization. Also, the stability of the scheme, i.e. the ability to suppress numerical errors is often only conditionally achievable, e.g. by limiting the time step size.

Cost-accuracy considerations

Every numerical discretization of transient (time-domain) wave equations results in numerical *dissipation* and *dispersion*, where the former describes the error in amplitudes, and the latter the error in phase due to the discrete grid. These errors grow with propagation distance such that one cannot simply propagate waves further away than in a previous example and achieve the same allowed target error, without reconsidering the spatio-temporal resolution. Since error estimates are not easily formulated for sophisticated methods, and no reference solution exists in complex media, this is no trivial matter but one every user of such methods should always be aware of.

As one may expect, different approaches are advantageous for different settings, and our three methods are a good basis for such trade-off considerations. A short summary of computational costs for different wave propagation problems is given in Table 7.1.

7.2 Numerical methods

We will give a brief overview of approaches that have been applied to the wave equation, and then forego most of them but focus on FD, FE, and FV, which are currently the most important numerical methods for global wave propagation. Furthermore, we will not discuss *absorbing boundaries*, but only delegate the interested reader to this very important asset to local-scale settings which is far from being solved. *Adaptive re-meshing* is another

	$f[\text{Hz}]$	$\Delta[\lambda^{-1}]$	DOF	RAM[GB]
hydrofracture monitoring	150	150	5×10^7	10
exploration seismology	30	300	2×10^9	300
seismic hazard	3	100	4×10^7	6
global body waves	0.15	300	2×10^9	300
multiple-orbit surface waves	0.005	150	4×10^8	70

Table 7.1: Grand challenges in computational seismology. From high to low frequencies f , propagation distance Δ as a number of wavelengths, degrees of freedom DOF (\sim grid points) and memory requirement RAM.

interesting aspect e.g. in fluid dynamics, but rendered useless in the context of global seismology given the quick global coverage of seismic waves due to reflections. We will also ignore *frequency-domain* methods, partly due to no known implementation for global wave propagation, but mostly due to the fact that these result in implicit schemes, thus become prohibitively expensive for broadband signals and impulsive sources.

Central to all numerical schemes is the *implementation*, including optimized cache access, domain decomposition, and parallel solutions. Several seismic methods have been tested on graphical processing units (GPUs), yielding accelerated performance up to two orders of magnitude. Also, the spectral-element method for global wave propagation is known to scale favorably on the largest supercomputers.

Overview of prominent approaches

Application areas of different numerical approaches, and their *specific stand-out properties*:

- **Finite differences.** Time-dependent PDEs, seismic wave propagation, geophysical fluid dynamics (mantle, atmosphere, oceans), Maxwell's equations, ground-penetrating radar. *Robust, simple concept, easy to parallelize, regular grids, explicit method.*
- **Finite elements.** Static and time-dependent PDEs, seismic wave propagation, statics, geophysical fluid dynamics, all problems. *Irregular geometry/grids, implicit/explicit approach, parallelizable, founded, more complex algorithms, engineering problems.*
- **Finite volumes.** Time-dependent PDEs, seismic wave propagation, mainly fluid dynamics. *Robust, simple concept, irregular grids, explicit method.*
- **Particle-based methods.** Lattice-gas methods, molecular dynamics, granular problems, fluid flow, earthquake simulations. *Very heterogeneous problems, nonlinear problems.*
- **Boundary-element methods.** Problems with boundaries (rupture), only discretization of planes. *Based on analytical solutions, good for problems with special boundary conditions (rupture, cracks, etc).*

- **Pseudospectral methods.** Orthogonal basis functions, spectral accuracy of space derivatives, wave propagation, ground-penetrating radar. *Regular grids, high accuracy/cost ratio, explicit method, problems with discontinuities & parallelization.*

7.2.1 Strong form and velocity-stress formulation

Let \mathbf{u} be a continuous displacement vector in an everywhere solid Earth model Ω bounded by $\partial\Omega$ and characterized by density ρ and elastic tensor \mathbf{c} . The linearized momentum equation due to an indigenous body-force excitation \mathbf{f} (representing earthquakes) in Ω reads

$$\rho \partial_t^2 \mathbf{u} - \nabla \cdot \boldsymbol{\tau} = \mathbf{f} \quad \text{in } \Omega \quad (7.1)$$

subject to the constitutive elastic stress-strain relationship (*Hooke's Law*)

$$\boldsymbol{\tau} = \mathbf{c} : \nabla \mathbf{u} \quad \text{in } \Omega, \quad (7.2)$$

and the dynamical free-surface boundary condition

$$\hat{\mathbf{n}} \cdot \boldsymbol{\tau} = \mathbf{0} \quad \text{on } \partial\Omega. \quad (7.3)$$

Eq. (7.1) is also known as a *strong form* of the equations of motion, as it is generally applicable without specifying boundary or initial conditions. It is furthermore a second-order differential equation (containing a Laplacian). One can rewrite the system as a first-order system in time as a *hyperbolic equation* with free variables velocity $\mathbf{v} = \partial_t \mathbf{u}$ and stress $\boldsymbol{\tau}$:

$$\rho \partial_t \mathbf{v} - \nabla \cdot \boldsymbol{\tau} = \mathbf{f} \quad (7.4)$$

$$\partial_t \boldsymbol{\tau} = \lambda (\nabla \cdot \mathbf{v}) \mathbf{I} - \mu (\nabla \mathbf{v} + \nabla \mathbf{v}^T), \quad (7.5)$$

i.e. a system of 9 equations. Solving for stress and velocity, there are no second derivatives to be undertaken as compared to the displacement solution in the second-order case, eq. (7.1).

7.2.2 Weak & variational form

Alternatively, one may construct the *weak form*, which is done via mean weighted residuals or variational principles as follows: Multiply the second-order system by a square-integrable, differentiable *test function* (also called cardinal function, virtual displacement) \mathbf{w} and integrate over the domain Ω such that

$$\int_{\Omega} \rho \mathbf{w} \cdot \partial_t^2 \mathbf{u} d^3 \mathbf{x} = \int_{\Omega} \mathbf{w} \cdot \nabla \cdot (\mathbf{c} : \nabla \mathbf{u}) d^3 \mathbf{x} + \int_{\Omega} \mathbf{w} \cdot \mathbf{f} d^3 \mathbf{x}. \quad (7.6)$$

Upon partial integration, one reduces the spatial differentiation in the first term on the right hand side,

$$\int_{\Omega} \rho \mathbf{w} \cdot \partial_t^2 \mathbf{u} d^3 \mathbf{x} = - \int_{\Omega} \nabla \mathbf{w} : \mathbf{c} : \nabla \mathbf{u} d^3 \mathbf{x} + \int_{\Omega} \nabla \cdot (\mathbf{w} \cdot \boldsymbol{\tau}) d^3 \mathbf{x} + \int_{\Omega} \mathbf{w} \cdot \mathbf{f} d^3 \mathbf{x}, \quad (7.7)$$

and apply Gauss' divergence theorem and utilize the traction-free surface boundary condition to eliminate

$$\int_{\Omega} \nabla \cdot (\mathbf{w} \cdot \boldsymbol{\tau}) d^3 \mathbf{x} = \int_{\partial\Omega} \mathbf{w} \cdot \hat{\mathbf{n}} \cdot \boldsymbol{\tau} d^2 \mathbf{x} = 0. \quad (7.8)$$

Just like the velocity-stress first-order system, remaining spatial derivatives are first order. Defining bilinear form $a(\mathbf{w}, \mathbf{u}) = \int_{\Omega} \nabla \mathbf{w} : \mathbf{c} : \nabla \mathbf{u} d^3 \mathbf{x}$ and inner product $(\mathbf{w}, \mathbf{u}) = \int_{\Omega} \mathbf{w} \cdot \mathbf{u} d^3 \mathbf{x}$ one can write this in compact notation as follows: Find $\mathbf{u} \in V$ such that for all $\mathbf{w} \in V$

$$(\mathbf{w}, \rho \ddot{\mathbf{u}}) + a(\mathbf{w}, \mathbf{u}) = (\mathbf{w}, \mathbf{f}), \quad (7.9)$$

where V is a Hilbert space spanning once-differentiable, piecewise continuous functions. The fundamental property of the weak form is that it is subjected to specific boundary conditions and naturally satisfies them upon discretization. Thus, it will prove useful especially for problems involving sharp boundaries, surfaces, or solid-fluid interfaces.

Galerkin weak form

This continuous form is seen as infinite-dimensional from a numerical perspective. To “down-dimensionalize” or discretize, one recasts this weak system in the Galerkin sense by choosing a subspace $V_n \subset V$ of dimension n to solve a projected problem: Find $\mathbf{u}_n \in V_n$ such that for all $\mathbf{w}_n \in V_n$ $(\mathbf{w}_n, \rho_n \mathbf{u}_n) + a(\mathbf{w}_n, \mathbf{u}_n) = (\mathbf{w}_n, \mathbf{f}_n)$, where the equation remains the same, but the function spaces have changed. One then recasts this into matrix form by expanding the solution onto a basis $\mathbf{e}_1, \mathbf{e}_2, \dots, \mathbf{e}_n$ of V_n as $\mathbf{u}_n = \sum_{i=1}^n \mathbf{u}_i \mathbf{e}_i$, insert this into the Galerkin weak form and obtain

$$\sum_i \ddot{\mathbf{u}}_i (\mathbf{e}_i, \rho \mathbf{e}_j) + \sum_i \mathbf{u}_i a(\mathbf{e}_i, \mathbf{e}_j) = \sum_i \mathbf{f}_i (\mathbf{e}_i, \mathbf{e}_j), \quad (7.10)$$

which is a linear system of equations and can be written in matrix form as

$$\mathbf{M} \ddot{\mathbf{u}} + \mathbf{K} \mathbf{u} = \mathbf{f}, \quad (7.11)$$

where $M_{ij} = \int_{\Omega} \rho \mathbf{e}_i \cdot \mathbf{e}_j d^3 \mathbf{x}$ and $K_{ij} = \int_{\Omega} \nabla \mathbf{e}_i : \mathbf{c} : \nabla \mathbf{e}_j d^3 \mathbf{x}$. Eq. (7.11) is an ordinary differential equation in time. Effectively, we have separated the initial problem into one of solving the spatial dependencies \mathbf{M} and \mathbf{K} given by the inner product $(.,.)$ and bilinear form $a(.,.)$, and a temporal evolution problem eq. (7.11). All element-based techniques rely on this system, as we will see later.

7.2.3 CFL stability criterion

Analyzing the behavior of a discrete system in space and time $(\Delta x, \Delta t)$ using harmonic functions, one can deduce a stability criterion of the form

$$C \frac{\Delta t}{\Delta x} \leq 1, \quad (7.12)$$

where C is a (constant) Courant stability number and depends on operator length, dimension, and numerical scheme. This condition is valid for a wide variety of schemes, including FD and FEM. Effectively, this criterion imposes a bound on the choices of spatial and temporal

discretization. Often, one constructs a spatial mesh based upon a target minimal period $T_0 = n_\lambda^0 \max \tau(\mathbf{x})$, where the characteristic lead time needed to propagate a wave through grid spacing Δx is defined as $\tau(\mathbf{x}) = \Delta x(\mathbf{x})/c(\mathbf{x})$ with c being the medium wavespeed. One then uses the stability condition to derive the necessary time step Δt as

$$\Delta t \leq C \min \tau(\mathbf{x}). \quad (7.13)$$

In unconditionally stable schemes (implicit), one can choose large time steps, which, even considering the iterative nature, may be beneficial in terms of the overall CPU time.

7.3 Finite differences

The *finite differences* method is in general easy to implement, efficient on supercomputers, but suffers large dispersion errors especially for waves sensitive to boundaries (surface waves, diffracted waves). This results from being based upon the velocity-stress strong form, i.e. the need to specifically impose boundary conditions which is often of lower accuracy order than the propagation scheme.

A finite difference operator is generally defined by truncating the Taylor series expansion of the definition of a functional derivative, e.g. in the *centered scheme* as

$$\partial_x \approx \frac{f(x + \Delta x) - f(x - \Delta x)}{2\Delta x}, \quad (7.14)$$

which, if we analyze the Taylor expansion, is of second-order accuracy (Δx^2). The chosen order of accuracy depends on problems, but in many cases a fourth-order scheme is applied. The 1D acoustic wave equation can then be solved as

$$p(t + \Delta t) = \frac{c^2 \Delta t^2}{\Delta x^2} [p(x + \Delta x) - 2p(x) + p(x - \Delta x)] + 2p(t) - p(t - \Delta t) + f dt^2. \quad (7.15)$$

This is an *explicit* scheme in time, i.e. no iterations are needed to update the pressure p . Finite differences and other schemes can be formulated as *implicit schemes* as well, in which these iterations are necessary, but with the advantage of unconditional stability.

Staggered grid

Very popular in the finite-difference community is the *staggered grid*, where material properties (ρ, \mathbf{c}) and wavefields $(\mathbf{v}, \boldsymbol{\tau})$ are defined on offset grids to reduce their difference operator. A sketch of such a staggered grid cell is shown in Fig. 7.1. Staggered-grids usually lead to higher accuracy and order convergence.

Optimally accurate operators

An improved formulation of finite-differences operators based upon minimizing their error can be devised as follows (Bob Geller, University of Tokyo):

Define the exact system as $\omega^2 (\mathbf{M}^0 - \mathbf{K}^0) \mathbf{u}^0 = -\mathbf{f}^0$, and the numerical system as $\omega^2 (\mathbf{M} - \mathbf{K}) \mathbf{u} = -\mathbf{f}$ in the frequency domain. Using the first-order Born approximation (weak scattering),

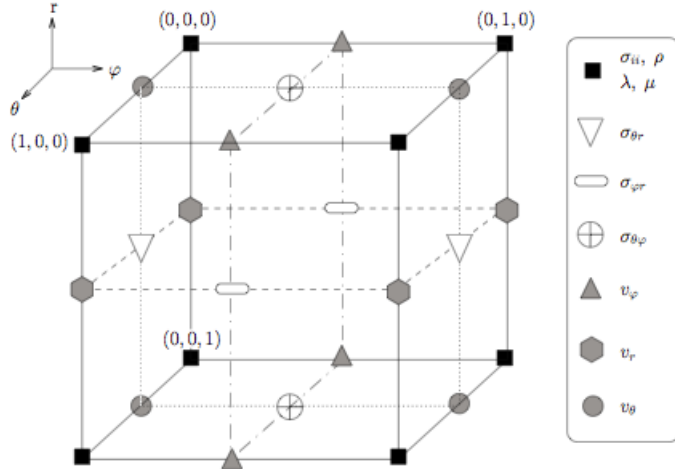


Figure 2.1: The unit cell for the staggered grid in spherical coordinates (for simplicity, the unit cell is drawn in cartesian geometry).

Figure 7.1: Finite-differences staggered grid

estimate the error of the solution as

$$\delta \mathbf{u} = -(\omega^2 \mathbf{M}^0 - \mathbf{K}^0)^{-1} (\omega^2 \delta \mathbf{M} - \delta \mathbf{K}) \mathbf{u}^0, \quad (7.16)$$

and expand the numerical solution in the normal mode basis with eigenfunctions \mathbf{u}_m as $\mathbf{u} = \sum_m c_m \mathbf{u}_m$, where c_m are the coefficients. The solution error is then defined in a relative sense as

$$\frac{\delta \mathbf{u}}{\mathbf{u}^0} = \left| \frac{\omega^2 \delta M_{mm} - \delta K_{mm}}{\omega^2 - \omega_m^2} \right| = |\delta M_{mm}| \left| \frac{\omega^2 - \delta K_{mm}/\delta M_{mm}}{\omega^2 - \omega_m^2} \right|, \quad (7.17)$$

where ω_m is the eigenfrequency, $\delta M_{mm} = \mathbf{u}_m^T \delta \boldsymbol{\tau} \mathbf{u}_m$ and $\delta K_{mm} = \mathbf{u}_m^K \delta \mathbf{K} \mathbf{u}_m$. Optimal accuracy may then be achieved by

$$\omega^2 \delta M_{mm} - \delta K_{mm} \approx 0. \quad (7.18)$$

This is an interesting approach since it embeds the minimization of the joint spatio-temporal error into the definition of the differential operator. You can find more information in the suggested literature.

In summary, the *finite differences* (FD) method is probably the most popular approach of numerically solving seismic wave propagation problems. This is mainly due to its relatively simple implementation. Additionally, the regular gridding of the mesh makes it computationally very fast, thus attractive for problems which need to solve wave propagations for many different sources and events. It is also well suited to parallelization, showing good scaling on large computers. Drawbacks are problems in accuracy when modeling media with irregular surfaces, such as e.g. surface topography. It needs special techniques to enforce the boundary conditions, making the implementation more complicated. Thus, accurately modeling surface waves may become a challenge for real media using finite differences.

Examples

Wave propagation in a spherical section:

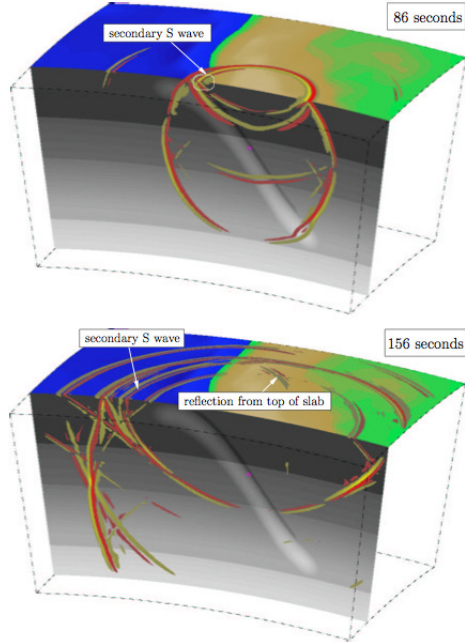


Figure 7.2: Vertical velocity snapshots of a low-velocity layer slab model at 7s dominant period. Top: wavefield after 86s; bottom: wavefield after 156s. The source location is denoted with a purple star (Nissen-Meyer, 2001).

Global axisymmetric SH wave propagation (2D equations):

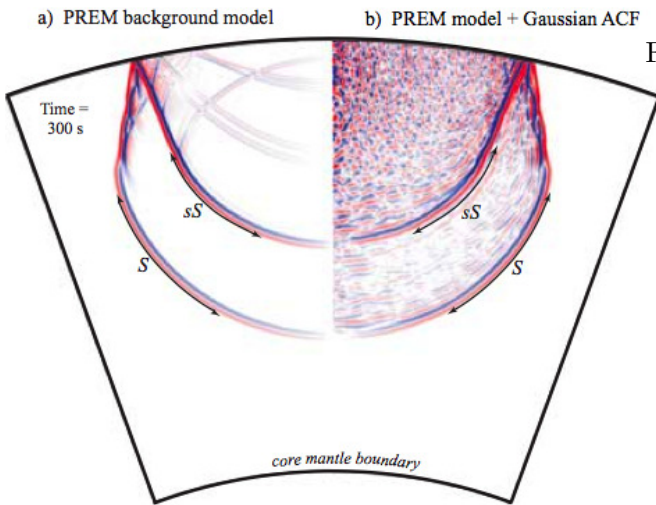


Figure 7.3: (a) The SH velocity wavefield for a 200-km-deep source in the PREM background model. The S and sS wavefronts are labelled. (b) The velocity wavefield at the same timestep as in panel (a) for the PREM model with random v_s variations applied. The random variations were created with a Gaussian autocorrelation function with corner wavelength of 32km and 3 percent rms v_s perturbations (from Jahnke et al., 2008).

Perpetrators: Heiner Igel (LMU Munich), Peter Moczo (Slovak Academy of Sciences, Bratislava), Michael Thorne (Univ. of Utah)

7.4 Finite & spectral elements

Finite element methods (FEM) enjoy a wide range of applications, most prominently in engineering (statics, fluid mechanics, thermoelasticity). Their prime advantage over finite differences is the geometric flexibility: While the FD operators assume constant Δx and thus a regular mesh, finite elements can be deformed radically, adhering to using the weak form. As such, one subdivides the integrals into non-overlapping “elements”, and computes all terms locally, then adds their edge & corner contributions up from all touching sides (*assembly*). This warrants also efficient parallelization, and the expansion of the system inside elements is flexible, as it is done upon a reference domain and all geometric complexity is contained in the Jacobian mapping function.

Mass and stiffness matrix

Recalling the weak form, we define the respective terms as:

$$\int_{\Omega} \left[\underbrace{\rho \mathbf{w} \cdot \partial_t^2 \mathbf{u}}_{\text{mass term}} + \underbrace{\lambda(\nabla \cdot \mathbf{w})(\nabla \cdot \mathbf{u}) + 2\mu \nabla \mathbf{w} : \mathbf{E}}_{\text{stiffness term } (\mathbf{w}^T \mathbf{K} \mathbf{u})} \right] d^3 \mathbf{x} = \begin{bmatrix} \text{single-force source term} \\ \underbrace{\hat{\mathbf{p}} \cdot \mathbf{w}(r_r \hat{\mathbf{z}}) \delta(t)}_{\mathbf{M} : \nabla \mathbf{w}(r_s \hat{\mathbf{z}}) H(t)} \\ \text{moment-tensor source term} \end{bmatrix} \quad \forall \mathbf{w} \in V_0.$$

The mass term containing the mass matrix \mathbf{M} is reminiscent of the kinetic energy, and the stiffness term containing the stiffness matrix \mathbf{K} of the potential or elastic energy. The crux of FEM lies in computing these spatial terms, which we will show after tackling the time evolution and meshing.

Temporal evolution

The resultant ordinary differential equation in time, eq. (7.11) $\mathbf{M}\ddot{\mathbf{u}}(t) + \mathbf{K}\mathbf{u}(t) = \mathbf{F}(t)$, is mostly solved using conventional centered finite-difference schemes (Newmark scheme), but more sophisticated methods have been tested as well, such as fourth-order Runge-Kutta or symplectic schemes. We depict two solutions to the ODE, the 2nd-order Newmark and a symplectic 4th-order scheme of superior accuracy:

\mathcal{O}^2 Newmark scheme:

$$\begin{aligned} \mathbf{u}_j &= \mathbf{u}_{j-1} + \Delta t \dot{\mathbf{u}}_{j-1} + \frac{1}{2} \Delta t^2 \ddot{\mathbf{u}}_{j-1} \\ \ddot{\mathbf{u}}_j &= \mathbf{M}^{-1} (\mathbf{F}_j - \mathbf{K}\mathbf{u}_j) \\ \dot{\mathbf{u}}_j &= \dot{\mathbf{u}}_j + \frac{1}{2} \Delta t [\ddot{\mathbf{u}}_{j-1} + \ddot{\mathbf{u}}_j] \end{aligned}$$

\mathcal{O}^4 symplectic scheme:

$$\begin{aligned} \mathbf{u}_j &= \mathbf{u}_{j-1} + \kappa_j \Delta t \dot{\mathbf{u}}_{j-1} \\ \dot{\mathbf{u}}_j &= \dot{\mathbf{u}}_{j-1} + \pi_j \Delta t \mathbf{M}^{-1} (\mathbf{F}_j - \mathbf{K}\mathbf{u}_j) \\ \mathbf{u}_5 &= \mathbf{u}_4 + \kappa_5 \Delta t \dot{\mathbf{u}}_4 \end{aligned}$$

$$j = 1, \dots, J = 4:$$

4-fold force evaluation per Δt

Meshing the globe

Meshing a sphere is a formidable challenge. The main issue lies in the problem that a spherical mesh decreases in size with depth, whereas seismic velocities increase, thus posing a doubly detrimental condition on meshing efficiency. Finite-element based methods required

continuous elements, i.e. each edge needs to be replicated on the other side such that one cannot simply divide the layering into fractions. Alternatively, mesh coarsening has gained most popularity. Even still, the center of the sphere is a singularity. To overcome this problem, one can place a cube at the center and define an analytical mapping between the two domains (see Figure 7.4). This leads to an efficient meshing of the globe using quadrilateral (2D) and hexahedral (3D) elements.

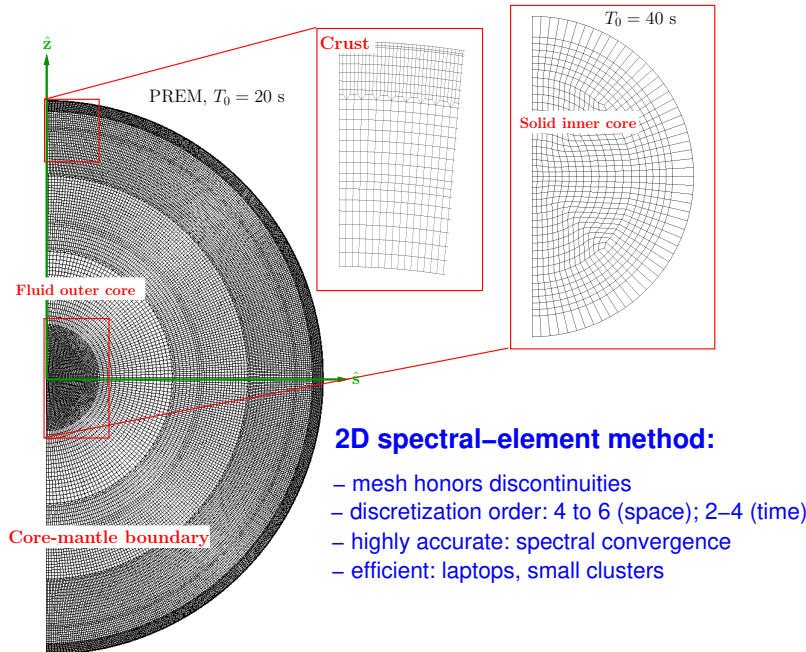


Figure 7.4: A PREM mesh for 20 second periods and an axisymmetric domain. Note 3 mesh coarsening levels, and a different topology in the center. (Nissen-Meyer et al., 2007).

Elements, geometric mapping, Jacobian

In FEM, one reverts geometric complexity to reference elements spanning $[-1, 1]^d$ (d : dimension), using the Jacobian \mathcal{J} which is simply the derivative matrix of physical with respect to reference coordinates (Fig 7.5).

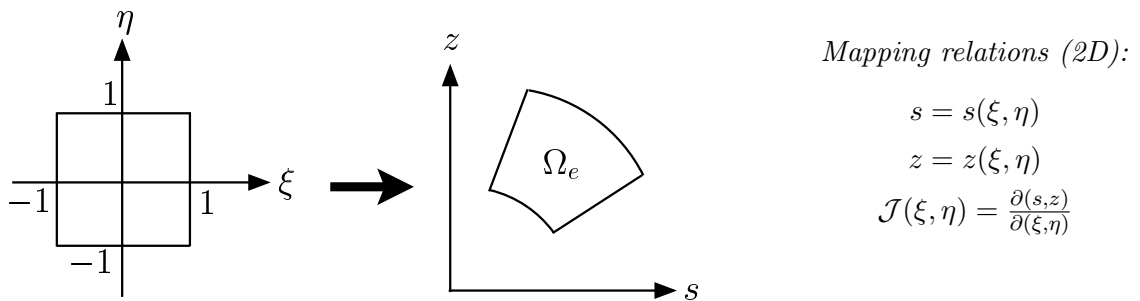
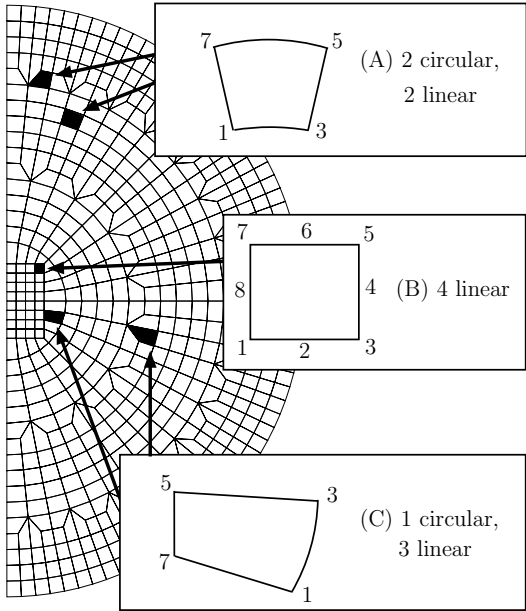


Figure 7.5: Mapping physical (distorted) elements to the reference frame.

For the domain depicted on the left of Figure 7.6, one has analytical transformation formulae,

given on the right:



$$s(\xi, \eta) = (1 + \eta) \tilde{s}_{\text{top}}(\xi) + (1 - \eta) \tilde{s}_{\text{bot}}(\xi)$$

$$\tilde{s}_{\text{top}}(\xi) = \frac{r_7}{2} \sin \left\{ \left[(1 - \xi) \frac{\theta_7}{2} + (1 + \xi) \theta_5 \right] \right\}$$

$$\tilde{s}_{\text{bot}}(\xi) = \frac{r_1}{2} \sin \left\{ \left[(1 - \xi) \frac{\theta_1}{2} + (1 + \xi) \theta_3 \right] \right\}$$

$$\tilde{s}_{\text{bot}}(\xi) = \frac{r_1}{4} [(1 - \xi) \sin \theta_1 + (1 + \xi) \sin \theta_3]$$

$$s(\xi, \eta) = \sum_{a=1}^8 N_a(\xi, \eta) s_a,$$

$$N_6(\xi, \eta) = (1 - \xi^2)(1 + \eta)/2$$

Figure 7.6: Element topology for a 2D global mesh. 3 distinct types are elucidated.

The Jacobian represents one of the most sensitive ingredients into numerical schemes as it contains all geometric information: Extremely deformed elements and angles often result in negative or extreme values for the Jacobian and therefore unstable regimes for simulations. Analyzing the robustness of the Jacobian is thus a valuable task after creating a mesh.

Gauss-Lobatto-Legendre basis & Gauss quadrature

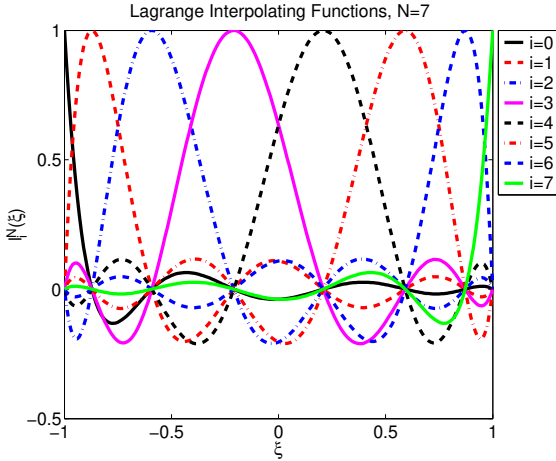
In the framework of *spectral elements*, one expands the functions within elements upon a Gauss-Lobatto-Legendre basis (e.g., of order 4 to 6), and approximates wavefields and test functions via *Lagrange interpolating functions*. Schematically, the procedure for *evaluating integrals* in 3D is

$$\int_{\Omega} \Psi(\mathbf{x}) d^3\mathbf{x} \Rightarrow \sum_e \int_{\Omega_e} \Psi(\mathbf{x}) d^3\mathbf{x} \Rightarrow \int_{-1}^1 \int_{-1}^1 \int_{-1}^1 \Psi(\xi, \eta, \gamma) \mathcal{J}(\xi, \eta, \gamma) d\xi d\eta d\gamma \quad (7.19)$$

where the Lagrange interpolating functions are given by

$$l_i^N(\xi) = \begin{cases} (-1)^N \frac{(1-\xi)P'_N(\xi)}{N(N+1)}, & i = 0, \\ \frac{1}{N(N+1)P_N(\xi_i^N)} \frac{(1-\xi^2)P'_N(\xi)}{\xi_i^N - \xi}, & 0 < i < N, \\ \frac{(1+\xi)P'_N(\xi)}{N(N+1)}, & i = N, \end{cases} \quad (7.20)$$

where P_N are Legendre polynomials of order N , and $-1 \leq \xi \leq 1$.



Field representation:

$$u(\xi, \eta) \approx \sum_{i,j,k=0}^N u_{ijk} l_i^N(\xi) l_j^N(\eta) l_k^N(\gamma)$$

Note: $l_i^N(\xi_p) = \delta_{ip}$ are orthogonal

Figure 7.7: Lagrange functions for 7th-order spatial discretization

One then inserts these representations into the weak form and integrates using Gauss quadrature

$$\int_{-1}^1 \Psi(\xi, \eta, \gamma) \mathcal{J}(\xi, \eta, \gamma) d\xi d\eta d\gamma \approx \sum_{pqr=0}^N \sigma_p \sigma_q \sigma_r \Psi(\xi_p, \eta_q, \gamma_r) \mathcal{J}(\xi_p, \eta_q, \gamma_r), \quad (7.21)$$

where $\sigma_p = \int_{-1}^1 l_p^N(\xi) d\xi$ are integration weights. This leads to explicit (and lengthy) expressions for the stiffness, force, and mass terms. Within this framework, the mass matrix is *diagonal by construction*, which is the basis for the above-mentioned explicit time marching schemes in which we pulled \mathbf{M} to the right hand side, a procedure often called *mass lumping*.

Note that other discretizations usually yield non-diagonal mass matrices which need to be inverted iteratively and cause significantly more communication across processors, a property not so desirable for large-scale problems.

In summary, the *spectral-element method* (SEM) is a very promising tool for seismic wave propagation due to a combination of geometric flexibility with a fast, explicit, easily parallelizable solver. Due to solving the weak form of the equations of motion, it is mathematically and numerically exact in dealing with seismic wave propagation along the free surface. Combined with its mesh flexibility, the method thus becomes highly accurate for modeling both body and surface waves. The one central drawback is that only rectangular elements yield an orthogonal system in the basis functions, which puts a limit to the geometric flexibility in that e.g. wedges cannot as easily be meshed as with triangle-based elements.

Examples

Global wave propagation comparing a spectral-element method with normal mode summation:

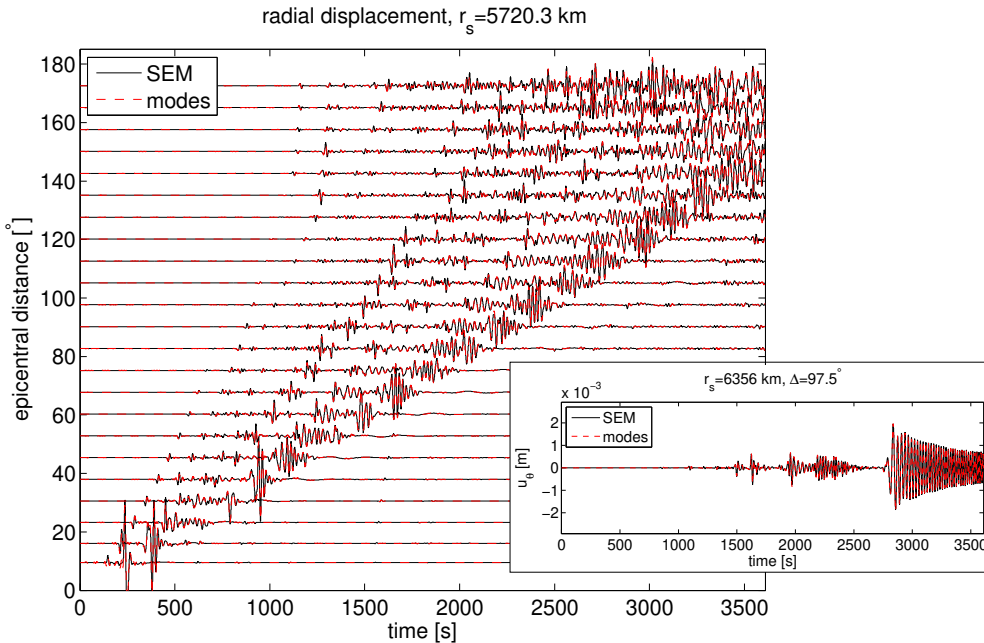


Figure 7.8: SEM solution versus normal mode summation for a PREM model. Left: deep source and globally distributed seismograms. Right: Crustal source resulting in dispersive surface waves. Mesh resolution: $T_0 = 9$ s, 721500 grid points, 35000 time steps (Nissen-Meyer et al., 2007).

A simulation of an overthrust model reminiscent of seismic exploration scales:

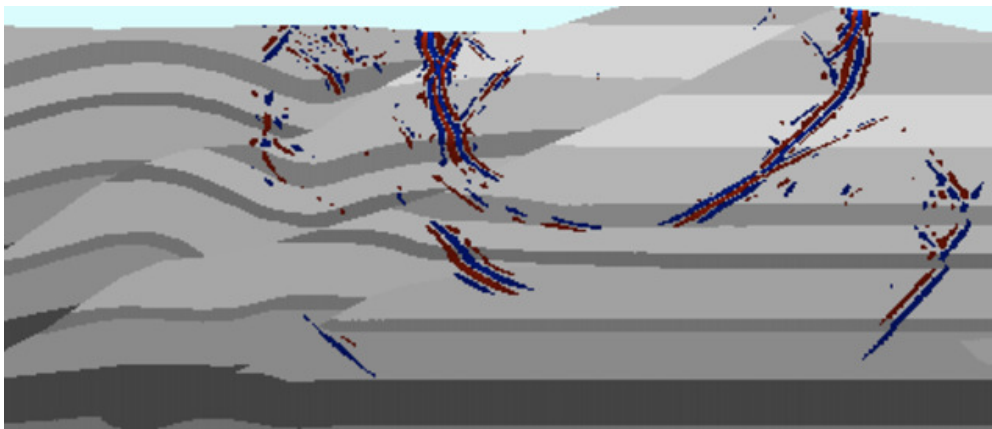


Figure 7.9: SEM solution snapshot of an overthrust model with many faults (SEG/EAGE benchmark model). Meshing such structures in 2D is straightforward.

Perpetrators: Dimitri Komatitsch (CNRS), Jean-Pierre Vilotte (IPG Paris), Emanuel Chaljub (LGIT Grenoble), Jeroen Tromp (Princeton), Tarje Nissen-Meyer (Oxford), Andreas Fichtner (ETH), Daniel Peter (KAUST)

7.5 Finite volumes & discontinuous Galerkin methods

Finite volume methods are based upon discretizing a volume around the location in question, applying the divergence theorem and defining the derivatives upon this volume. Instead of going into details on this method which has only been partially prominent in seismology due to issues with interfaces, we briefly describe the most sophisticated numerical technique presented here: the *discontinuous Galerkin* (DG) method.

This fairly recent approach is based upon the velocity-stress system, but discretizing its weak form with discontinuous basis functions and allowing for triangular element topologies. Thus, one can easily accommodate wedges and most complex structures unlike the SEM. The disadvantage of the DG methods is its numerical cost which exceeds that of the SEM by 1-2 orders of magnitude.

Tetrahedral meshing

Meshing using tetrahedra (3D) and triangles (2D) is algorithmically solved: Many packages exist that can accommodate any structure in such meshes, unlike for the rectangular case. This puts the discontinuous Galerkin method into a promising position to tackle the most heterogeneous structures, which shall be of increasing importance in future computational seismology, despite the increased cost of the simulations compared to other methods.

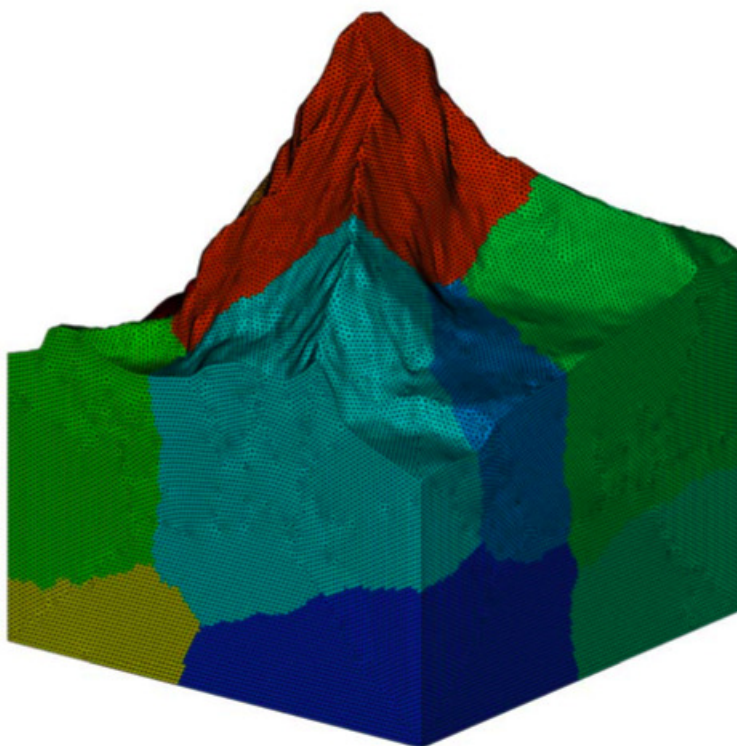


Figure 7.10: Matterhorn mesh. Such structures can only efficiently be accommodated by triangular/tetrahedral meshing such as done in the discontinuous Galerkin method (courtesy Martin Käser).

Global wave propagation with the DG approach has been undertaken in 2D, and is under way in 3D: no principal obstacles prevent this application from being a fruitful addition to the only other available solver for 3D earth models, the spectral-element method. The latter is however very efficient at these scales, partly due to the fact that 3D tomographic models

at the global scale are smooth, and sharp interfaces purely spherical (plus topography), a setting which is well tractable by hexahedral meshing.

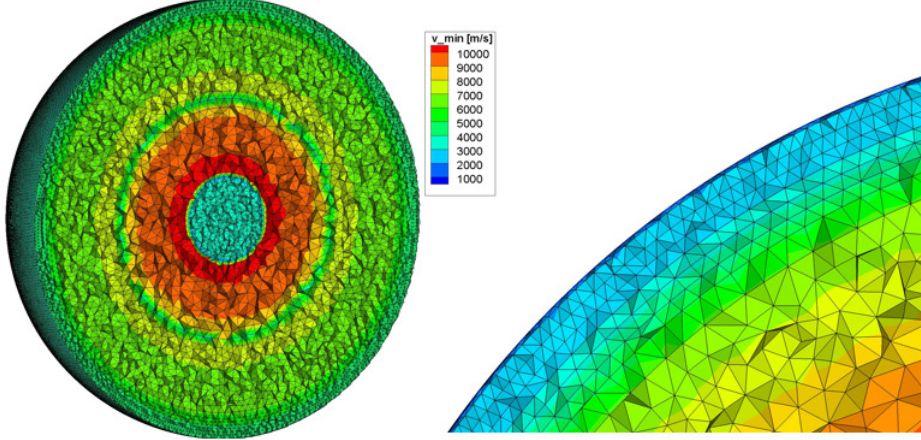


Figure 7.11: Meshing of the globe using triangles. Many commercial and open-source meshing softwares exist to generate such meshes very quickly, unlike for the rectangular case (courtesy Martin Käser).

Numerical fluxes

The velocity-stress system can be conveniently compacted to

$$\partial_t \mathbf{Q} + (\mathbf{A} \partial_x + \mathbf{B} \partial_y + \mathbf{C} \partial_z) \mathbf{Q} = 0, \quad (7.22)$$

where the unknowns have been concatenated into the 9-component vector $\mathbf{Q} = (\boldsymbol{\tau}, \mathbf{v})$, and $\mathbf{A}, \mathbf{B}, \mathbf{C}$ are space-dependent Jacobian matrices of size 9×9 containing (sparsely populated) entries on material properties, and their eigenvalues determine the propagation velocity of the waves. The discretization upon expanding the unknowns with polynomials as $Q_p(\xi, \eta, \gamma, t) = \hat{Q}_{pl}(t)\Phi_l(\xi, \eta, \gamma)$ is achieved similarly to the FE framework discussed above, safe for the modification that the tiling into elemental integrals is done before the integration by parts. This effectively results in so-called *numerical flux* terms F which accommodate the conditions at and across the element walls:

$$\int_{\tau} \Phi_k \partial_t Q_p d^3 \mathbf{x} + \int_{\partial\tau} \Phi_k F_p^h d^2 \mathbf{x} - \int_{\tau} (\partial_x \Phi_k A_{pq} Q_q + \partial_y \Phi_k C_{pq} Q_q + \partial_z \Phi_k B_{pq} Q_q) d^3 \mathbf{x} = 0, \quad (7.23)$$

where fluxes have a generic form

$$F_p^h \sim \frac{1}{2} T_{rs} (A_{qr} + |A_{qr}|) T_{rs}^{-1} \hat{Q}_{sl} \Phi_l, \quad (7.24)$$

$|A_{qr}|$ are matrices containing the eigenvalues, and T_{rs} are rotation matrices to align the unknowns with the element edges.

While the expansion of unknowns into piecewise polynomials Φ_k is similar to FE, they do not need to be continuous across boundaries, and no global assembly is necessary, thus yield-

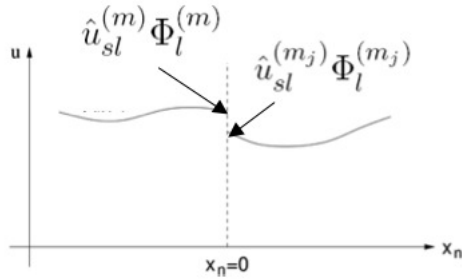


Figure 7.12: Discontinuous displacement discretization at element boundaries in the DG method (courtesy Martin Käser).

ing a completely local system well suited for parallelization. Time evolution is done upon polynomial coefficients instead of cell averages (as in the finite volume method) such that no polynomial reconstruction is necessary, and realized using the so-called ADER approach of arbitrarily high approximation orders. For more details, you can follow the literature given at the end of this section.

In summary, the *discontinuous Galerkin* (DG) method is a very versatile and highly accurate numerical method. Its superb flexibility in terms of meshing highly complex media, e.g. with strong topography and/or internal interfaces such as geological faults, make it very attractive for numerically solving seismic wave propagation on complicated local-scale problems. Additionally, the locality of the discretization and the explicit treatment of numerical fluxes across element boundaries is well suited for modeling dynamic rupture propagation on complex faults on large supercomputers.

Examples

Dynamic rupture simulation for the Landers earthquake:

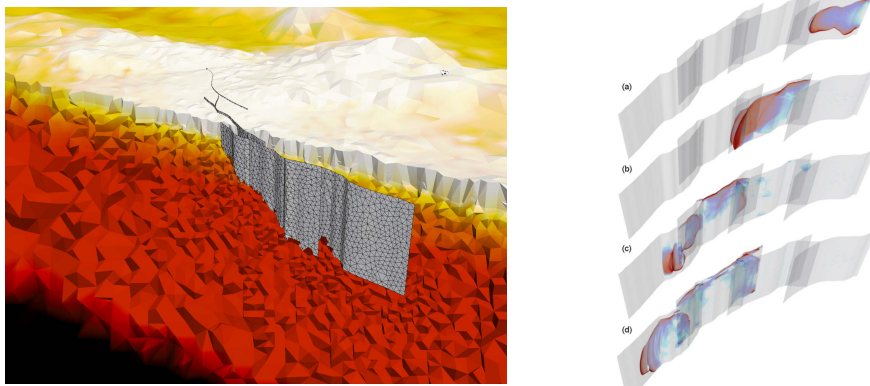


Figure 7.13: Left: Tetrahedral mesh for the Landers faults, Right: time snapshots of dynamic rupture propagation showing maximum slip rate on the fault (Heineke et al., 2014).

Peak ground motion simulations honoring topography and local sedimentary basins:

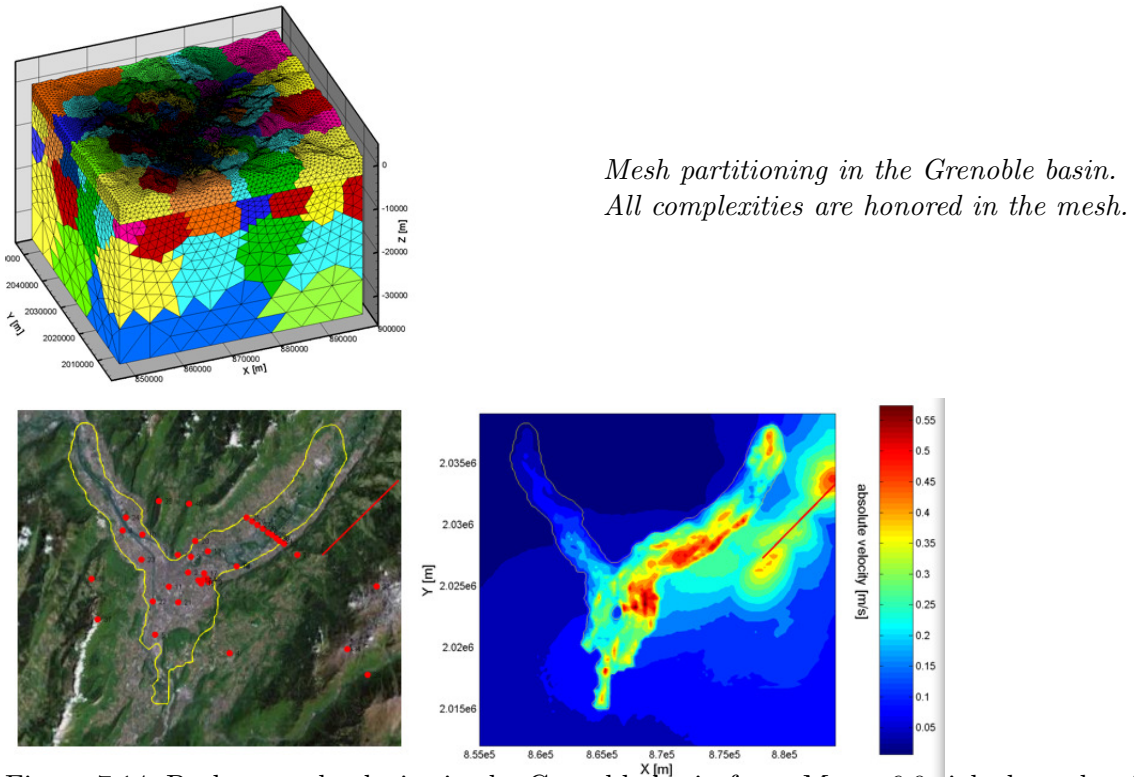


Figure 7.14: Peak ground velocity in the Grenoble basin for a $Mw = 6.0$ right-lateral strike-slip event, showing trapped waves (courtesy Martin Käser).

Perpetrators: Alice-Agnes Gabriel, Christian Pelties, Martin Käser (LMU Munich)

7.6 Conclusions

We showed that complex media can only be solved with fully numerical techniques. Assuming the methods are sufficiently accurate, what is the actual scientific purpose for global seismology? The answer is two-fold:

1. Forward modeling (trial-and-error),
2. A basis for inverse problems (Green's function, sensitivity kernels).

Many applications exist on both ends, where the former focuses more on specific data sets and regions in the Earth, and researchers manipulate certain parameters of the setting (model, source-receiver configuration) to find solutions that best fit the data. This has been useful for confirming many findings in the lowermost mantle such as big thermo-chemical piles underneath Africa and the Pacific, or ultra-low velocity zones. Inverse problems on the other hand form an entirely different set of problems and are dealt with in other courses.

To conclude, it is necessary to have a solution to the forward problem for each reference model in the inverse approach, and if done properly using full-wave theory, then a solution is needed at each potential scattering, or model point in the domain. This is a gigantic computational task, ranking amongst the most challenging issues for supercomputing across all disciplines, and ranging from global inversions to seismic imaging at the exploration scale. With the advance of these methods hand in hand with exponential increase in computational power and quality seismic data, this is one of the most evolving and promising fields of seismology and geophysics.

Further reading

Literature:

- G. Cohen, 2002. *Higher-Order Numerical Methods for Transient Wave Equations*, in: Scientific Computation. Springer Verlag.
- Geller, R.J., and Takeuchi, N.: {1995, Geophys.J.Int., 123,449-470; 1998, Geophys.J.Int., 135,48-62.}
- Heineke, A. et al., 2014. *Petascale High Order Dynamic Rupture Earthquake Simulations on Heterogeneous Supercomputers*, in SC14: International Conference for High Performance Computing, Networking, Storage and Analysis.
- Käser, M., and M. Dumbser, 2006. *An Arbitrary High Order Discontinuous Galerkin Method for Elastic Waves on Unstructured Meshes I: The Two-Dimensional Isotropic Case with External Source Terms*, Geophys. J. Int., 166(2), 855-877
- Komatitsch, D., and Tromp, J., 1999. *Introduction to the spectral element method for three-dimensional seismic wave propagation*, Geophys. J. Int., 139, 806-822.
- Komatitsch, D., Tsuboi, S., and Tromp, J., 2005. *The spectral-element method in seismology*, in Seismic Earth: Array Analysis of Broadband Seismograms, AGU Monograph, editors A. Levander and G. Nolet.
- Tromp, J., 2007. *Forward modeling and synthetic seismograms: 3D numerical methods*, in Treatise on Geophysics, editors B. Romanowicz and A. Dziewonski, Elsevier.

Web resources:

Spectral-element method:

Codes: [SPECFEM3D_GLOBE](#), [SALVUS](#), [AxiSEM](#)

Computational Infrastructure in Geodynamics: <http://www.geodynamics.org>

ShakeMovie & global seismicity: <http://shakemovie.princeton.edu>

Finite-differences method:

Codes: [AWP](#), [SW4](#), [SOFI3D](#), [Terrae motus](#), [Nuquake](#)

SPICE open source code library: <http://www.spice-rtn.org>

QUEST open source code library: <http://www.quest-itn.org>

Discontinuous Galerkin method:

Codes: [SeisSol](#), [EDGE](#)